

## Biophysical Studies of Biomimetic Bone Cement with Alginate for Applications in the Biomedical Field

Jamilah Abed Al-Harhi

Ministry of Education || KSA

**Abstract:** Osteoporosis and many other bone defects are described as the diseases that have attracted attention in the past two decades over worldwide. Because of it is known as a silent disease and with a high commonness rate among the elderly, the battle could be difficult. This paper aims to assess the impact of the inclusion of some additions to the brushite cement and use fluid simulation in the body that contain calcium and free of protein in the laboratory as a stimulant for the apatite formed such as bone apatite samples consisting of brushite cement and various elements that have been added to the roofs. The research paper adopted the experimental approach. The stable phases of calcium phosphate cements depend significantly upon temperatures and the presence of water, either during processing or in the use situation. At body temperature, only two calcium phosphates are stable when in interaction with aqueous media such as body fluids. The samples under investigation are used to select samples which can be considered suitable as a biomaterial in vitro. The samples prepared in the form of two samples each one regards with a group of additives including sodium Alginate, Wollastonite, Titanium Oxide, Hydroxyapatite and Zinc Oxide. Soaking brushite samples with their additives in simulated body fluid for one week may cause presence of a bone-like apatite layer phase  $(Ca_{10}(OH)_2(PO_4)_6, HA)$  on the surface of these samples. To sustain the aim of the study, the samples studied by using the X-ray diffraction spectra, scanning electron microscope and Raman spectroscopy. The X-ray diffraction used to ensure the presence of the components used in the preparation of the samples is present in the samples or not. The study of X-ray examination for the samples under investigation after soaking for one week in SBF to help us to recognize new phases appearing after the interaction between the samples surfaces and the components of the SBF.

**Keywords:** Biophysical, Biomimetic Bone, Alginate, Biomedical field, Biomaterials, Brushite, Hydroxyapatite, Sodium Alginate, Wollastonite

## دراسات بيوفيزيائية للمحاكاة البيولوجية لإسمنت العظام مع الألبينات لاستخدامه في المجال الطبي

جميلة عابد الحارثي

وزارة التعليم || المملكة العربية السعودية

**المستخلص:** تعتبر هشاشة العظام والعديد من عيوب العظام الأخرى بأنها الأمراض التي جذبت الانتباه في العقدين الماضيين في جميع أنحاء العالم. نظرًا لأنه يُعرف بالمرض الصامت وبنسبة انتشار عالية بين كبار السن، فقد تكون المعركة صعبة. تهدف هذه الورقة إلى تقييم أثر إدراج بعض الإضافات على إسمنت البروشيت واستخدام محاكاة السوائل في الجسم التي تحتوي على الكالسيوم والخالي من البروتين في المختبر كمحفز للأباتيت المتكون مثل عينات الأباتيت العظمي المكونة من إسمنت البروشيت وعناصر مختلفة تمت إضافتها إلى الأسطح. اعتمدت الورقة البحثية المنهج التجريبي. تعتمد المراحل المستقرة من إسمنت فوسفات الكالسيوم

بشكل كبير على درجات الحرارة ووجود الماء، سواء أثناء المعالجة أو في حالة الاستخدام. عند درجة حرارة الجسم، يكون اثنان فقط من فوسفات الكالسيوم مستقرين عند التفاعل مع الوسائط المائية مثل سوائل الجسم. تُستخدم العينات قيد البحث لاختيار العينات التي يمكن اعتبارها مناسبة كمواد حيوية في المختبر. العينات المحضرة على شكل عينتين تتعلق كل واحدة بمجموعة من الإضافات بما في ذلك ألجينات الصوديوم، والولاستونيت، وأكسيد التيتانيوم، والهيدروكسيباتيت، وأكسيد الزنك. قد يتسبب نقع عينات البروشيت مع إضافتها في simulated body fluid لمدة أسبوع واحد في وجود مرحلة طبقة الأباتيت الشبيهة بالعظام (6 (PO4) 2 (OH) 2 (Ca10, HA) على سطح هذه العينات. لدعم هدف الدراسة، تمت دراسة العينات باستخدام أطياف حيود الأشعة السينية والميكروسكوب الإلكتروني ومطياف رامان. إن حيود الأشعة السينية المستخدم لضمان وجود المكونات المستخدمة في تحضير العينات موجود. دراسة الفحص بالأشعة السينية للعينات قيد التحقيق بعد النقع لمدة أسبوع في SBF يساعد على التعرف على المراحل الجديدة التي تظهر بعد التفاعل بين أسطح العينات ومكونات SBF.

الكلمات المفتاحية: الفيزياء الحيوية، المحاكاة الحيوية، الألجينات، المجال الطبي الحيوي، المواد الحيوية، البرشيت، هيدروكسيباتيت، ألجينات الصوديوم، ولاستونيت.

## I. Introduction.

Osteoporosis and many other bone defects are described as the diseases that have attracted attention in the past two decades over worldwide (Pouresmaeili et al., 2018; Kweon et al., 2018). Because of it is known as a silent disease and with a high commonness rate among the elderly, the battle could be difficult (Gao et al., 2019). The situation is no different in the Kingdom of Saudi Arabia (KSA) for the rest of the world (Olic-Akrapovic, Radic, Tonkic, 2021). Many of the results of epidemiological and statistical analyzes showed that 34 % of Saudi women and 30.7 % of Saudi men in the age range between 50- 79 years are infected with osteoporosis (Sadat Ali et al., 2012). So, this rate is expected to increase in the average age of the population in Saudi Arabia in between 65 to 75 through years 2013 and 2020. Therefore, it is probable to spread occurrence of osteoporosis even higher level as a result of the increase of the average of the age (Murat et al., 2021). Based on that it should be considered in many studies are needed to overcome these challenges facing the bones of the elderly in the years ahead and also the available therapeutic ways. Especially for those patients who do not have the opportunity to get the bone by natural ways from themselves or relatives of some of them (Scimeca et al., 2018). Therefore, it is essential to think of alternative ways to overcome the lack of availability of these bones, the lack of these bones availability or replace it with material that could be the work of renewal of the cells of the bone or that materials using in filling the gaps resulting from these diseases (DiNicolantonio et al., 2018). This thesis is targeting the contribution of some in vitro results for alternative ways to get bone substitutes through laboratory studies to confirm the possibility of using under the available treatment conditions. There are many factors that play an important role in the high prevalence of the disease, including the rate of change in the lifestyle of the Saudi citizen, with a lack of calcium intake and lack of physical activity, and the high prevalence of vitamin A deficiency rate (d), and are among the main reasons (Mirza, Canalis, 2015). As a result, stats hospitals in Saudi Arabia, there are nearly 8768 hip fractures annually cost the

state many billions of Riyals, and being endemic area to a lack of vitamin D, bone health has become a serious concern in Saudi Arabia (Alwahhabi, 2015).

Repair of bone or bone renewal has many problems in the formation of bone during a surgical procedure. Every year, millions of people in the world, Saudi Arabia suffer from a defect in the bone as a result of congenital defects or exposure to accidents or diseases such as bone cancer and the lack of availability of a perfect bone for compensation. So, the trend has been directed to manufacture of alternative materials represented in the different types of bio-cement derived from calcium phosphate and which one's brushite cement. Brushite cement is one of the types of cement dynamic promising and through research and studies in the past two decades, which can be such a conclusion that this cement can be used in many critical areas, for example, to fill the bone diseased as well as the transfer of drugs into the vital objects in many biomedical uses. This cement can also serve as one of the sources of calcium ions and phosphate ions as well as to prepare for remineralization in solid tissue level studies laboratory. These successive studies have indicated that the brushite cement is one of biomaterials that can be used which has a unique feature on the cement of calcium phosphate and other systems is its ability to resorption under different physiological conditions. Biomaterial studies have resulted in the original formula for brushite cement and that she was able to make it brushite cement and known curse that cannot be dealt with easily handle as well as lower cohesion and compatibility with life bioactivity. This cement can also serve as one of the sources of calcium ions and phosphate ions as well as to prepare for remineralization in solid tissue level studies in-vitro.

This paper aims to assess the impact of the inclusion of some additions to the brushite cement and use fluid simulation in the body that contain calcium and free of protein in the laboratory as a stimulant for the apatite formed such as bone apatite samples consisting of brushite cement and various elements that have been added to the roofs. The investigation of the ability of this transformation to apatite like bone in the presence of calcium and skim protein goal of this paper, laboratory and which used many of the approved scientific instruments for these studies to make sure of the precipitation of the apatite on the surfaces of the samples under study.

## II. Methodology.

The research paper adopted the experimental approach. The stable phases of calcium phosphate cements depend significantly upon temperatures and the presence of water, either during processing or in the use situation. At body temperature, only two calcium phosphates are stable when in interaction with aqueous media such as body fluids. At  $\text{pH} < 4.2$ , the stable phase is brushite or dicalcium phosphate dihydrate (DCPD,  $\text{CaHPO}_4 \cdot 2\text{H}_2\text{O}$ ), while at  $\text{pH} \geq 4.2$  the stable phase is calcium phosphate ( $\text{Ca}_{10}(\text{HPO}_4)_6(\text{OH})_2$ ). Stoichiometric HA containing hydroxyl ions are stable mineral over the neutral and basic pH range (Ranter, et. el., 1996, Tamimi, et al, 2012, Tas and Bhadue, 2004). Accordingly, brushite is easily

hydrolyzed to the more stable phases of Octacalcium phosphate (OCP) and apatite under physiological conditions (Monma, et al., 1987) and (Madsen, 2008).

Brushite and hydroxyapatite crystals are prepared according to the flowchart shown in Figure (1). The starting material for preparing brushite and hydroxyapatite is di-ammonium hydrogen orthophosphate ((NH<sub>4</sub>)<sub>2</sub>HPO<sub>4</sub>, Merck, 99%, Chemical Abstracts Service (CAS) # 7783-28-0, Darmstadt, Germany) and calcium nitrate tetra hydrate (Ca (NO<sub>3</sub>)<sub>2</sub>·4H<sub>2</sub>O), Merck, 99.95 % CAS # 13477-34-4, Darmstadt, Germany). All chemicals were used as received from manufacturer without any additional purification. A diluted solution of ammonium hydroxide (NH<sub>4</sub>OH, CAS# 1336-21-6, Sigma Aldrich, St. Louis, MO, USA) and hydrochloric acid (HCl, CAS# 7647-01-0, Sigma Aldrich, St. Louis, MO, USA) were used as adjusting reagents for pH values. Two different groups of samples were prepared using the same procedure, namely co-precipitation method. All the preparation processes were done in the presence of double distilled water.

The samples used in this study were prepared starting from polymer alginate solutions that were obtained by using double distilled water. A cylindrical form made from stainless steel as molds with radius = 2 mm and height = 3 mm for shaping the samples of brushite and brushite /polymer composites. Sodium Alginate (Na-ALG) (C<sub>6</sub>H<sub>9</sub>NaO<sub>7</sub>), CAS # 9005-38-3, Sigma Aldrich, St. Louis, MO, USA) solution was added drop-wise to achieve the appropriate concentration of Ca (NO<sub>3</sub>)<sub>2</sub>·4H<sub>2</sub>O as crosslinking solution. The pH values of both solutions were set at different values ranging from 4 to 6, using HCl or NaOH (0.2 M), in order to evaluate the effect of the pH on the synthesis of the composite. Cross-linked brushite-alginate was occurred in the form dough. The dough was reserved in the crosslinking solution for 24 h to complete the crosslinking process and enable the growth of di-calcium phosphate into the dough. In order to eliminate excess Ca<sup>2+</sup> ions and other impurities, the dough was subjected for washing in distilled water. Finally, the dough was dried at room temperature for 24 h and then kept at constant temperature (50 °C) overnight (Dabiri et al., 2016).

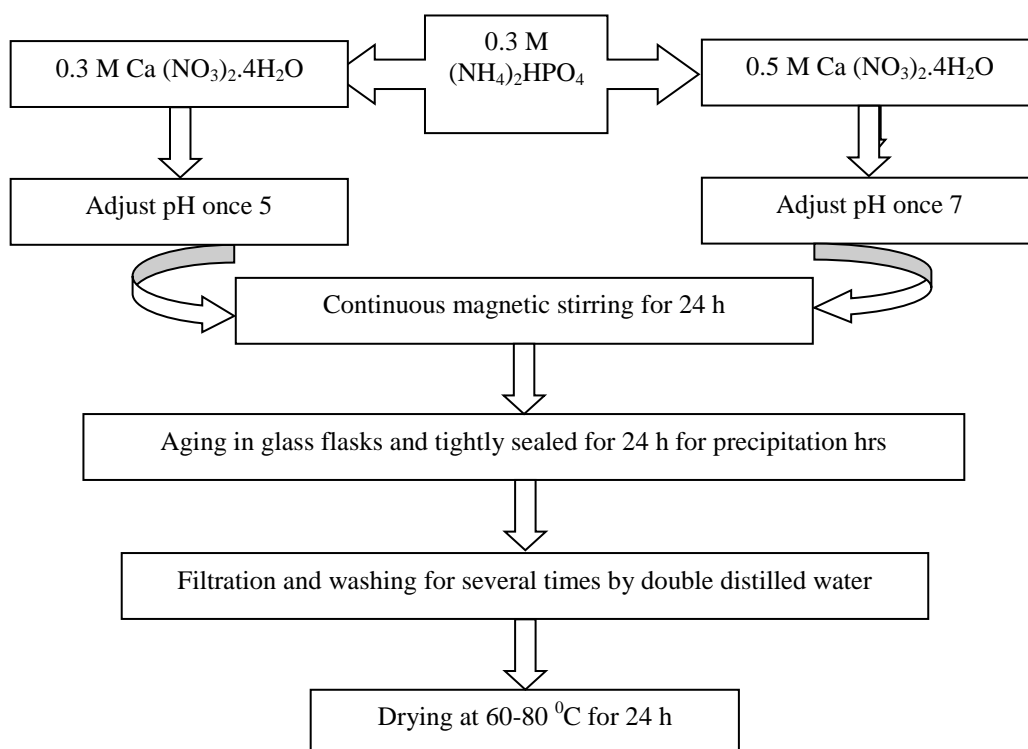


**Figure (1) Block diagram of the prepared brushite and hydroxyapatite powders**

To study the impact of the stage of the addition of different ions from the minerals to the dough which consisting of Brushite-Alginate (BR-ALG) was prepared. Many samples were prepared from the BR-ALG dough with different concentration from those ionic elements. The actual solution volume was determined by the amount necessary to ratio was selected based on workable consistency after a series of optimization studies. The additives elements were used are hydroxyapatite (HA, homemade), Titanium oxide (TiO<sub>2</sub>, powder, 99.8% trace metals basis, CAS # 12167-74-7, Sigma-Aldrich, St. Louis, MO, USA), zinc oxide (ZnO, Analytical standard, CAS # 1314-13-2, Sigma-Aldrich, St. Louis, MO, USA), Wollastonite (CaSiO<sub>3</sub>), Shanghai CNPC powder material Co., Ltd China (Mainland).

**Table (1) All detailed information concerning the samples and their preparation concentrations used in this study**

	Brushite Alginate	Alginate	Wollastonite	Titanium oxide	Zinc oxide	Hydroxyapatite
Sample (S1)	70 %	20 %	5 %	3 %	0 %	2 %
Sample (S2)	70 %	20 %	5 %	3 %	2 %	0 %

In vitro assessments were carried out by soaking the samples in simulated body fluid (SBF) for one week and incubating them at 37 °C until the time of the experiment. An SBF with ions composition nearly equal to blood plasma was prepared as previously reported (Kokubo et al., 1990; Juhasz et al., 2008). All highly purity reagents and other solvents were used without further purification.

The samples were prepared to characterization with using X-ray diffraction, Raman spectroscopy and the scanning electron microscopy and EDS.

## II.1 Physicochemical characterization of materials:

### X-Ray diffraction (XRD):

The progress of the growing the crystalline phases on the samples surface were traced by XRD to characterize the crystalline/amorphous nature of the samples and to identify any crystalline phases grown after soaking in SBF for one week. The samples were analyzed recording the XRD (Bruker D8 Advanced, USA), Cu-K $\alpha$  radiation and a nickel filter. XRD scanning was performed with a step size of 0.1° per step, 1 s per step and the scan range between  $2\theta = 20^\circ$  to  $70^\circ$ . The voltage used during the experiment was 40KV/40 mA.

### Scanning electron microscopy (SEM) and Energy dispersive spectroscopy (EDS)

The morphological investigation on the samples' surfaces (before and after soaking in SBF for one week) was achieved by scanning electron microscopy (SEM, Japan Electron Optics Laboratory (JEOL), JEOL Scanning Microscope 6360LV Tokyo Japan) was working at accelerated voltage of 15 KV, before being examined by SEM, the samples were gold coated using Hitachi coater. Energy dispersive X-ray spectrometer (EDS) (SEM-EDX, FESEM Jeol JSM-7600F) JEOL USA) provides elemental analysis in order to visualize the appearance of a bone-like apatite layer on their surfaces.

### Raman spectroscopy:

The samples of brushite, alginate and Wollastonite with their ionic additives were placed on a polished metal surface on the stage of DXR SmartRaman spectrometer (Thermo Scientific Redoks LAB, Ankara, Turkey). The Raman spectra were excited by highly polarized light at 633 nm and collected at a nominal resolution of  $2\text{ cm}^{-1}$  and a precision of  $1\text{ cm}^{-1}$  in the range between 50 to  $3500\text{ cm}^{-1}$ . Data acquisitions on the samples were done with the highest magnification with accumulation to improve the signal-to-noise ratio in the spectra.

### Bioactivity examinations:

The bioactivity investigation in vitro has been done through using simulated body fluid (SBF). The SBF was prepared at laboratory, with ions concentration nearly equal to human blood plasma. The SBF composition and preparation were previously described by (Kokubo and Takadama 2006) and (Kokubo et al. 1990). The samples were soaked in SBF for one week at  $37^\circ\text{C}$ . The samples were removed from SBF, then gently washed with distilled water and dried at room temperature.

### III. Results.

Figure (2) shows that there are many data peaks from the sample contains (BR +ALG) of X-ray diffraction spectrum that can used to compare between the spectrum comes out from the as-prepared sample and the spectrum of the brushite as a foundation material for comparison to be sure the samples containing brushite in its chemical structure (Dabiri et al. 2016).

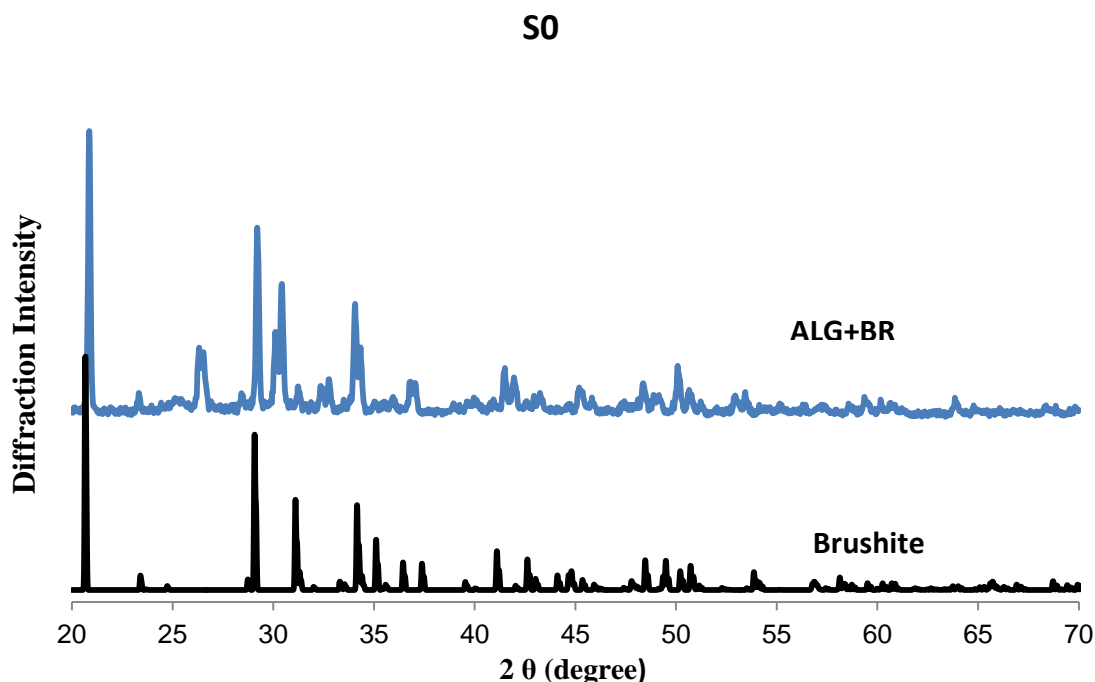


Figure (2) the XRD pattern for S0 (BR +ALG) to investigate the presence of the brushite in the as-prepared samples in comparison with BR according to the RRUFF database.

The X-ray diffraction pattern for S1 (Alginate, Brushite, Wollastonite, Hydroxyapatite and Titanium Oxide) shows the attendance of many peaks which belongs to Brushite; Wollastonite, Titanium Oxide  $Ti_2O$ , and Hydroxyapatite also which are registered in Table (2). The X-ray diffraction analysis was utilized to detect the phases change and the compounds for the sample. The collected data before and after reveal that there are no clear differences in the spectrum without more extra peaks are found. The presence of the hydroxyapatite at the surface of the S1 after soaking in SBF of one week period was examined. The data collected after soaking was compared with RRUFF database for the standard X-ray data of hydroxyapatite. The spectrum tells us that there is no clear studied transformation into hydroxyapatite because the sample itself contains hydroxyapatite and did not help to appear more extra peaks as a consequence of the compounds as a result due to soaking in SBF. Accordingly, the spectrum shows that there is a reason of this transformation to hydroxyapatite, but these changes have not been established to us because of the overlap underneath other peaks regarding to basically the presence of

hydroxyapatite in the sample composition. Also, there are no additional peaks formed due to the interaction between the sample compounds and the SBF for a period of one week. Table (2) summarizes the peak position, relative intensity, d-spacing and the Miller's indices for the data collected from figure (3) after soaking in one week in SBF. The table (2) tells the chemical components relative to each peak position and also the peak position underneath of the other components.

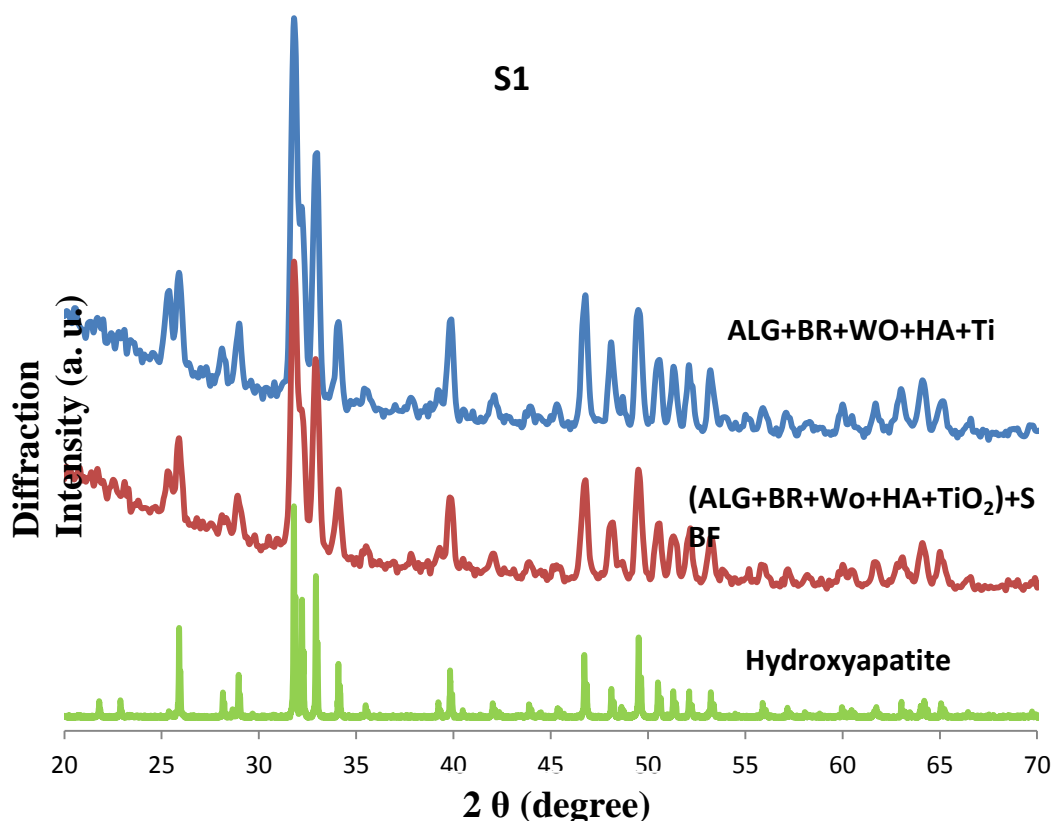


Figure (3) the X-ray spectrum of Alginate with Brushite cement, Wollastonite, Titanium Oxide and Hydroxyapatite (S5) before and after soaking in SBF for one week comparing with the standard database of Hydroxyapatite from RRUFF database.

Table (2) summarize the peak data for S5 (ALG+BR+WO+HA+TiO<sub>2</sub>)

Chemical component	2θ°	Int. %	d Å	h	k	l
	25.4	37	3.512	1	3	0
Wollastonite	25.9	41	3.438	-1	-3	1
Hydroxyapatite	28.1	23	3.169	1	0	2
Brushite	29.0	29	3.069	-1	4	1
Brushite	31.8	100	2.795	1	2	1
Hydroxyapatite	31.8 WO	100	2.777	0	0	2
Brushite Hydroxyapatite	33.0	69	2.688	-1	3	2

Chemical component	$2\theta^\circ$	Int. %	d Å	h	k	l
	33.0	69	2.720	3	0	0
Brushite	34.1	30	2.623	0	2	2
Hydroxyapatite	34.1	30	2.629	2	0	2
Wollastonite	35.4	14	2.534	-2	2	2
Wollastonite	37.8	12	2.383	-4	-2	1
Hydroxyapatite	39.2	14	2.296	2	1	2
Hydroxyapatite	39.8	29	2.261	0	1	1
Brushite	42.1	13	2.148	-2	4	2
Wollastonite	46.8	35	1.940	-2	-4	3

The X-ray spectrum of S2 (Alginate, Brushite, Wollastonite, Titanium Oxide and Zinc Oxide) shows the appearance of many peaks which belongs to Brushite, Titanium Oxide  $TiO_2$ , and Zinc Oxide also which are recorded in Table (3). By employing the X-ray diffraction analysis for this sample there is notice occurring in some changes for the peaks and also presence of more peaks in the compounds the sample. The data reveal that there are changes in phases due to the soaking in the SBF. These changes include the disappearance for some of the peaks such as peaks at  $2\theta = 24.7^\circ, 35.2^\circ, 38.1^\circ$  and  $59.1^\circ$  which belongs to  $TiO_2$  and WO respectively. This may attribute probably to that these elements were liquefied in the SBF. Likewise, the relative intensity of some peaks in the spectrum of the sample after soaking is increased. The presence of the hydroxyapatite on the surface of the S6 after soaking in SBF of one week period was examined. The data collected after soaking was compared with RRUFF database for the standard X-ray data of hydroxyapatite. The spectrum under investigation expressed to us that there are some changes that have overlap led to the emergence some of hydroxyapatite peaks underneath the peaks from brushite, Wollastonite, titanium oxide. These peaks located at angles  $31.8^\circ, 32.9^\circ, 34.08^\circ, 39.82^\circ, 49.52^\circ, 50.5^\circ, 51.28^\circ, 52.1^\circ$  and  $53.22^\circ$ . There is one peak at  $47.6^\circ$  is not belong to of any components of the sample. This result may attribute to the interaction of the sample ions with different ions contributed in the SBF.

S2

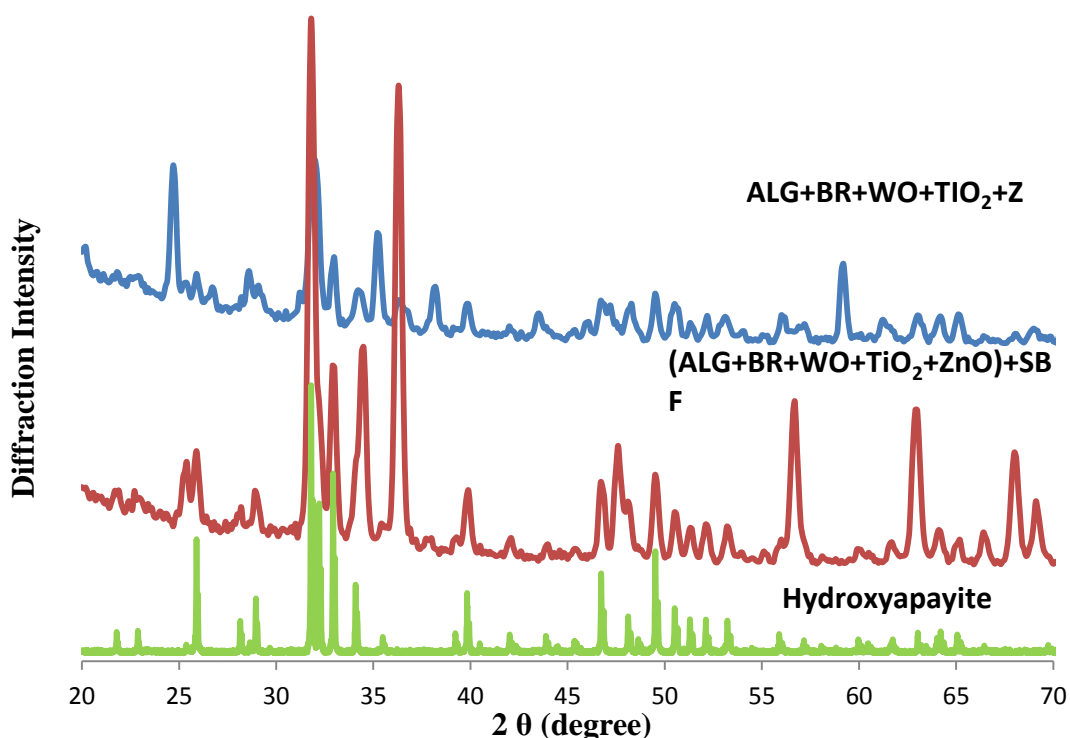


Figure (4): the X-ray spectrum of Alginate with Brushite cement, Wollastonite, Titanium Oxide and Zinc Oxide (S6) before and after soaking in SBF for one week comparing with the standard database of Hydroxyapatite indexed from RRUFF database.

Table (3) the peak position for S6

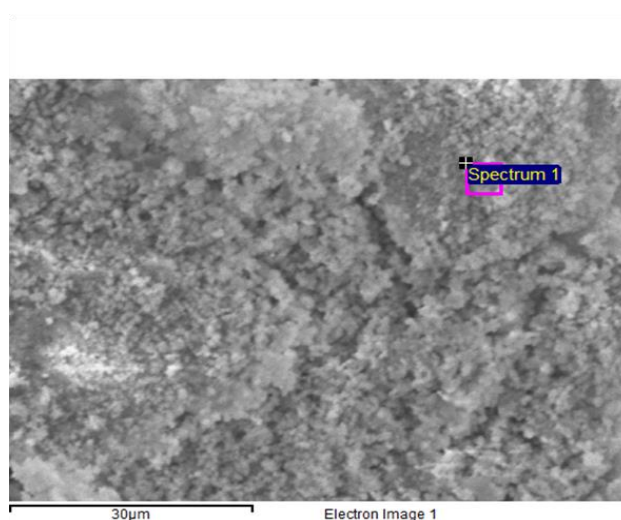
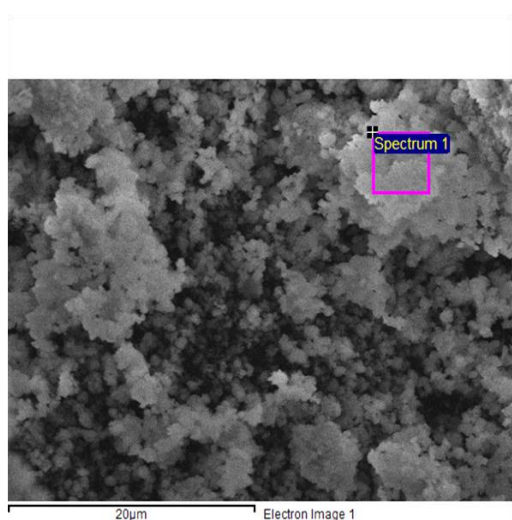
Chem. Compt.	2θ°	Int. %	d Å	h	k	l
Titanium Oxide	24.7	97	3.596	1	0	1
Wollastonite	25.3	37	3.518	-2	2	0
Wollastonite	25.9	41	3.438	-1	-3	1
Wollastonite	26.7	34	3.318	-1	3	0
Wollastonite	27.4	24	3.246	3	1	0
Wollastonite	28.2	29	3.185	-2	2	1
Brushite Hydroxyapatite	28.7	43	3.104	-1	1	2
	28.9	5.0	3.104	1	2	0
Brushite	29.1	35	3.069	-1	4	1
Brushite	32.0	100	2.795	0	0	2
Hydroxyapatite	32.0	100	2.777	1	1	2
Brushite	33.0	49	2.688	-1	3	2
Hydroxyapatite	33.0	49	2.720	3	0	0
Brushite	34.2	33	2.623	0	2	2
Hydroxyapatite	34.2	33	2.629	2	0	2

Chem. Compt.	2θ°	Int. %	d Å	h	k	l
Brushite	35.2	62	2.554	2	0	0
Zinc Oxide	36.3	28	2.4763	1	0	1
Titanium Oxide	38.2	35	2.3594	1	1	2
Hydroxyapatite	39.8	26	2.2633	3	1	0
Hydroxyapatite	46.7	27	1.9326	2	2	2
Wollastonite	48.3	26	1.8847	-4	-4	2

### III.1 SEM-EDS sample analysis

Table (4) Main Calcium Phosphate compounds (BarrÈre et al., 2006)

Name	Formula	Ca/P	Symbol
Monocalcium phosphate Monohydrate	Ca (H <sub>2</sub> PO <sub>4</sub> ) <sub>2</sub> H <sub>2</sub> O	0.50	MCPM
Dicalcium Phosphate	CaHPO <sub>4</sub>	1.00	DCP
Dicalcium Phosphate Dihydrate	CaHPO <sub>4</sub> .H <sub>2</sub> O	1.00	DCPD
Octacalcium phosphate	CaH <sub>2</sub> (PO <sub>4</sub> ) <sub>6</sub> .5H <sub>2</sub> O	1.33	OCP
Precipitated Hydroxyapatite "Tricalcium Phosphate"	Ca <sub>10-x</sub> (HPO <sub>4</sub> ) <sub>x</sub> (PO <sub>4</sub> ) <sub>6-x</sub> (OH) <sub>2-x</sub>	1.50-1.67	PHA
Amorphous Calcium phosphate n=3-4.5;15-20%H <sub>2</sub> O	Ca <sub>3</sub> (PO <sub>4</sub> ) <sub>2</sub> . n H <sub>2</sub> O	1.50	ACP
Monocalcium phosphate	Ca (H <sub>2</sub> PO <sub>4</sub> ) <sub>2</sub>	0.50	MCP
α-Tricalcium phosphate	α-Ca <sub>3</sub> (PO <sub>4</sub> ) <sub>2</sub>	1.50	α-TCP
β-Tricalcium phosphate	β-Ca <sub>3</sub> (PO <sub>4</sub> ) <sub>2</sub>	1.50	β-TCP
Sintered hydroxyapatite	Ca <sub>5</sub> (PO <sub>4</sub> ) <sub>3</sub> OH	1.67	HA
Oxyapatite	Ca <sub>10</sub> (PO <sub>4</sub> ) <sub>5</sub> O	1.67	OXA
Tetracalcium phosphate	Ca <sub>4</sub> (PO <sub>4</sub> ) <sub>2</sub> O	2.00	TetCP



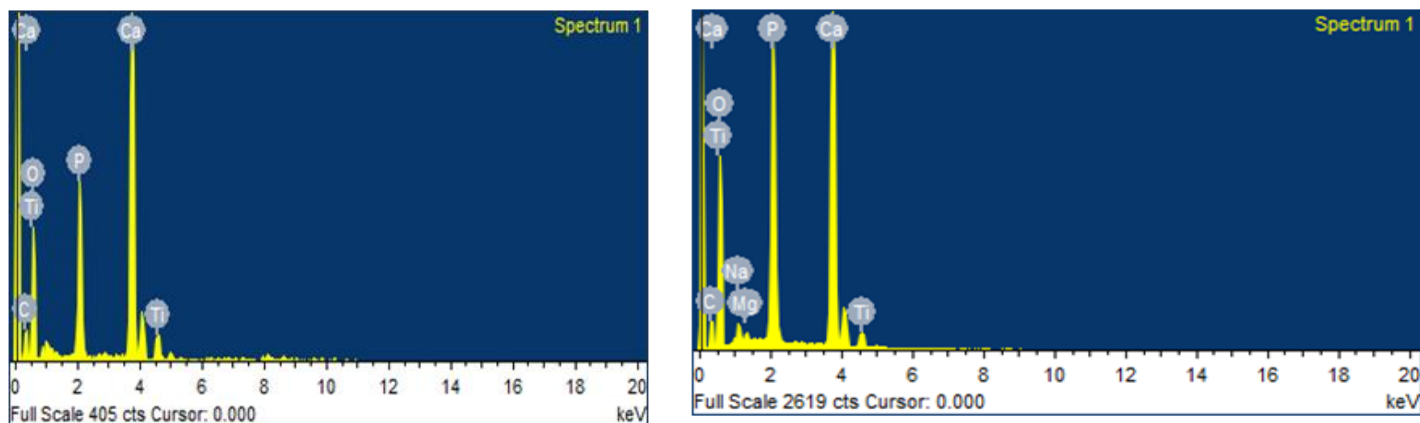


Figure (5) SEM-EDS profile of the surface of S1 before and after soaking in SBF for one week period

Table (5): The EDS elemental analysis data for sample S1 before and after soaking in SBF for one week period

Before Soaking					After Soaking				
Alginate+ Brushite + wollastonite +hydroxyapatite+TiO <sub>2</sub>					Alginate+ Brushite+wollastonite +hydroxyapatite+TiO <sub>2</sub>				
Element	Weight%	Atomic%	Ca/P		Element	Weight%	Atomic%	Ca/P	
C K	6.9	12.68			C K	7.04	12.5		
O K	41.96	57.87	3.48	weight	O K	44.07	58.74	1.86	weight
P K	10.46	7.45	2.69	atomic	P K	15.84	10.91	1.43	atomic
Ca K	36.35	20.01			Ca K	29.4	15.64		
Ti K	4.32	1.99			Ti K	2.4	1.07		
					Na K	0.88	0.81		
					Mg K	0.36	0.32		
Totals	100				Totals	100			

Figure (5) shows the SEM images and the EDS graphs of the sample S1 before and after soaking in SBF. The EDS detected Ca, P, O and C, among which the C out of the polymer matrix (Alginate) and CaCO<sub>3</sub> (carbonate apatite) after immersion in SBF, O comes from SiO<sub>2</sub>, the P from brushite, Ca and Si from Wollastonite and Ti out from TiO<sub>2</sub>. After soaking of the S5 in SBF for one week the images show real change in the morphology on sample surfaces in the SEM images were observed. The EDS noticed minor amounts of Na and Mg from the composition of SBF and Wollastonite, calcium silicate mineral (CaSiO<sub>3</sub>), that may comprise minor quantities of iron, magnesium, and manganese replacing for calcium, in totaling to Ca, P, O and C this may explain the presence of the Mg ions in the EDS data. The EDS elements analysis for S1 reveals that the Ca/P ratio of the atomic% is 2.69 before SBF and they are similar as those after

soaking, but the Ca/P atomic ratio drastically changed to 1.43 (reasonable value) as it is demonstrated clearly in table (5). By comparing the value of atomic ratio with the values of table (4) reveals the presence of precipitated hydroxyapatite and/or amorphous calcium phosphate, which contains minor components of magnesium (Takadama et al., 2008), on the surface of the sample (Madsen, 2008).

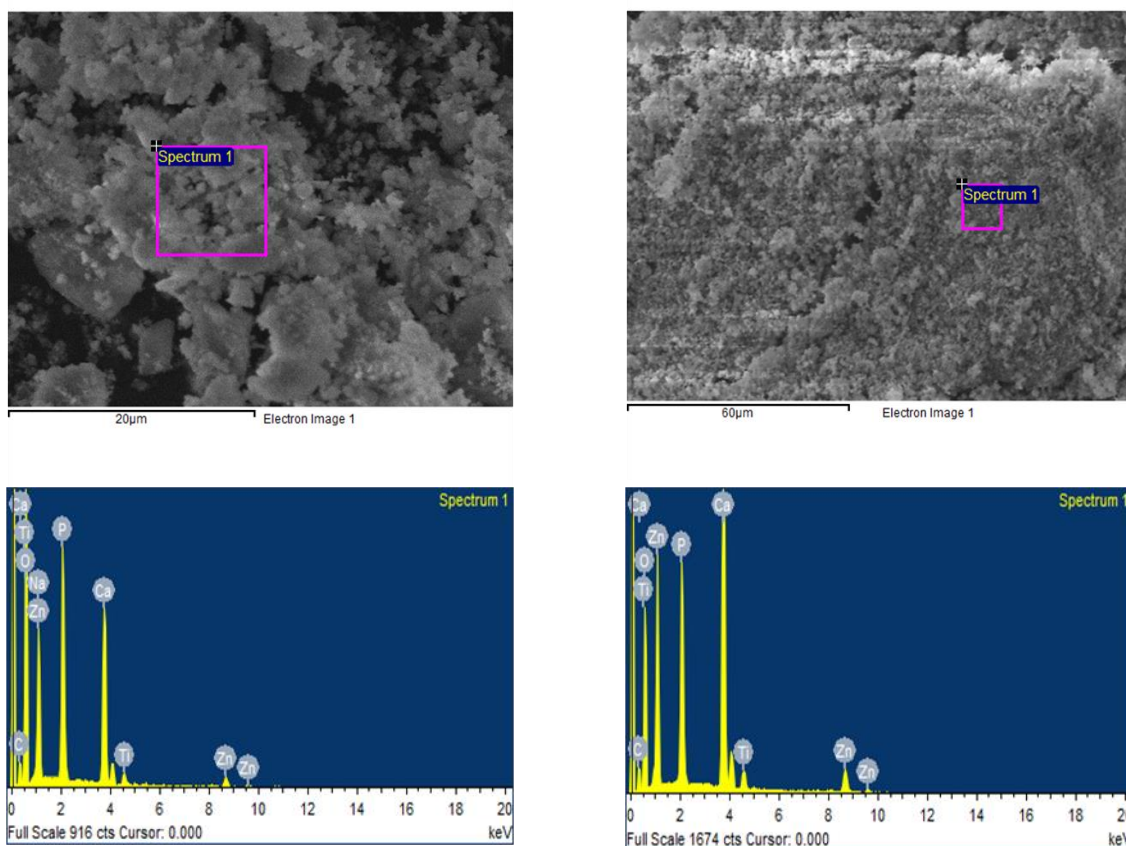


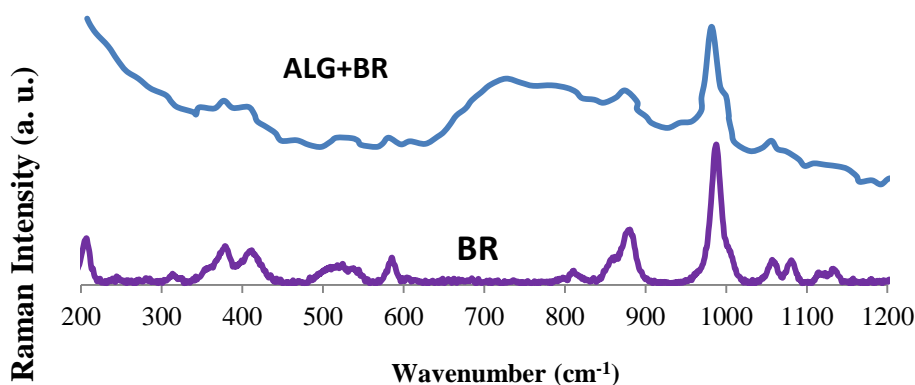
Figure (6): SEM-EDS profile of the surface of S2 before and after soaking in SBF for one week period

Table (6): The EDS elemental analysis data for sample S2 before and after soaking in SBF for one week period

Before Soaking				After Soaking			
Alginate+Brushite+wollastonite				Alginate+Brushite+wollastonite			
+TiO <sub>2</sub> +ZnO				+TiO <sub>2</sub> +ZnO			
Element	Weight%	Atomic%	Ca/P	Element	Weight%	Atomic%	Ca/P
C K	7.03	12.13		C K	6.24	12.92	
O K	47.89	62.03		O K	34.4	53.5	
Na K	6.23	5.61		missed	missed	missed	
P K	12.94	8.66	1.23	P K	11.22	9.01	2.19
Ca K	15.91	8.23	0.95	Ca K	24.56	15.25	1.69
Ti K	1.5	0.65		Ti K	2.44	1.27	
Zn L	8.51	2.7		Zn L	21.15	8.05	
Totals	100			Totals	100		

Figure (6) displays the SEM images and the EDS graphs of the sample S2 before and after soaking in SBF. The EDS perceived Ca, P, O and C, the carbon atom out of the polymer matrix (Alginate) and  $\text{CaCO}_3$  (carbonate apatite); O arises from  $\text{SiO}_2$ , the P from brushite and Ca from Wollastonite in addition to Ti from titanium oxide and Zn from Zinc oxide. The elemental analysis for S2 clears that the Ca/P ratio of the atomic% is 0.95. After soaking of the S6 in SBF for one week realize change in the morphology of sample surface which illustrates aggregation on the surface of the sample and small of the mill-fractured on surface of the sample particle appeared in the SEM images. The calculated value of the Ca/P ratio drastically changed to 1.69 as it is demonstrated clearly in table (6). The Ca/P atomic% ratio after soaking in SBF for S2 is approach the stoichiometric composition of hydroxyapatite which makes this sample is a perfect specimen for use as a biomaterial can be applied in-vitro (Grover et al., 2003).

### III.2 Raman spectroscopic analysis



**Figure (7): the Raman spectrum of Alginate with Brushite cement component comparing with the standard database of Brushite as indexed from RRUFF database.**

Figure (7) describes the relation between the wave numbers and the Raman intensities for the sample which contain the Alginate and brushite cement together. There are many signatures Raman peaks that used to compare between the collected spectra from the as-prepared sample (ALG+BR) and the spectrum of the brushite as foundation material from database of RRUFF (785 nm source). The comparison between the Raman spectrum of S0 and RRUFF database of brushite revealed that there are consistency between the sample's spectrum and the spectrum of brushite which can be summarized in table (7). All the data represented in the table (7) gives the position of the standard data tops brushite given database RRUFF compared to data collected from the Raman spectra of the S0 (ALG + BR) with the assignment of each peak. The data also includes spectrum located at the wavenumber  $988.60 \text{ cm}^{-1}$ , which is considered the fingerprint of brushite spectrum, also a complete assignment for all vibration modes that belong to each peak positions were addressed in table (7) (Xu et al. 1999), (Xu 1996) and (Forst et al. 2012).

Table (7): the main Raman peaks associated to measured data of Brushite in comparing with RRUFF database and the assignment of the modes of vibrations

Peak position for RRUFF standard	Peak position for measured spectrum	Int., %	Vibration modes
206.95	209.00	32	lattice vibration
245.00		4	$PO_4^{3-}$ bending $\nu_2''$
313.95	323.00	7	Missed
380.27	383.00	27	H <sub>2</sub> O translation
412.60	414.00	23	$PO_4^{3-}$ bending $\nu_2'$
512.20	525.00	11	$PO_4^{3-}$ bending $\nu_4''$
585.60	588.00	18	$PO_4^{3-}$ bending $\nu_4''$
809.20	795.00	8	out-of-plane (POH)
859.90	860.00	18	out-of-plane (POH)
880.00	880.00	38	P-O (H) $\nu_3'''$
988.60	987.00	100	$PO_4^{3-}$ stretching $\nu_1$
1055.30	1060.00	16	$PO_4^{3-}$ stretching $\nu_3''$
1081.20	1083.00	16	$PO_4^{3-}$ stretching $\nu_3''$
1117.70	1118.00	7	$HPO_4^{2-}$ stretching $\nu_3'$
1133.80	1131.00	10	$HPO_4^{2-}$ stretching $\nu_3''$

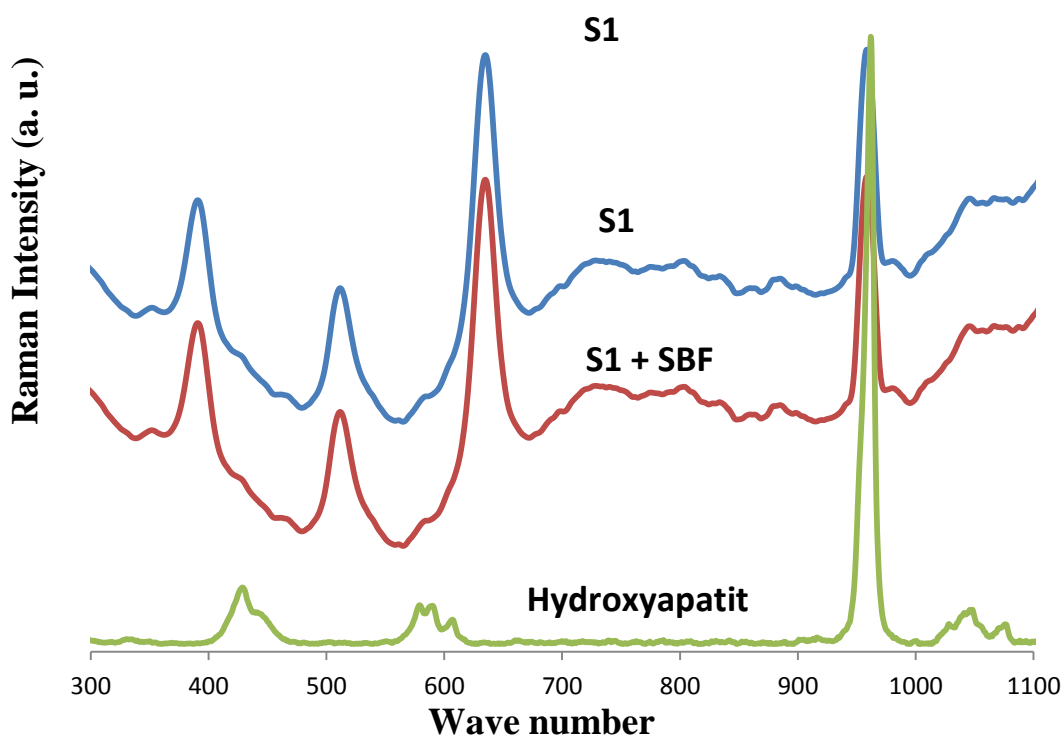


**Figure (8): the Raman spectrum of Alginate with Brushite cement, Wollastonite, Titanium Oxide and Hydroxyapatite (S1) before and after soaking in SBF for one week comparing with the standard database of Hydroxyapatite from RRUFF database**

Figure (8) shows the dependable Raman spectrum of the measured for the sample before, the second due to the soaked in SBF and the last for the Hydroxyapatite RRUFF database. Table (8) analyses the Raman peak position and their intensity percentages before and after soaking in SBF. The data belongs to the sample before soaking reveal 12 peaks are observed at 344.8, 390.4, 511.9, 580.8, 635.3, 730.7, 807.4, 852.8, 883.7, 958.3, 980.5 and 1046.1  $\text{cm}^{-1}$ , respectively. The peak at 390.4  $\text{cm}^{-1}$  belongs to (B<sub>1g</sub> vibration mode) TiO<sub>2</sub> and 511.9  $\text{cm}^{-1}$  is belonged to PO bending vibration mode of brushite and/or (A<sub>1g</sub>, B<sub>1g</sub> vibration modes) TiO<sub>2</sub>, the peak at 580.8  $\text{cm}^{-1}$  is belongs to brushite or hydroxyapatite. The peaks at 635.3  $\text{cm}^{-1}$  is assigned to Si-O stretch vibration modes of Wollastonite and/or (E<sub>g</sub> vibration mode) of TiO<sub>2</sub> (Hardcastle, 2011) and (Balachandran and Error, 1982) table (4-10), while the peaks at 807.4  $\text{cm}^{-1}$  assigned as brushite 883.70  $\text{cm}^{-1}$  assigned as brushite (P-O (H)). While these can be assigned peaks such as 958.30  $\text{cm}^{-1}$  to hydroxyapatite stretching, peak at 1041.1  $\text{cm}^{-1}$  are assigned to of hydroxyapatite. The peaks at 344.8, 730.7 and 852.2  $\text{cm}^{-1}$  are not identified till know (to our knowledge) and need more evaluation. To read more about symmetry and ant-symmetry vibration modes of titanium oxide refers to (Ishioka and Petek, 2012).

Data collected after soaking the sample for period of one week in the SBF revealed fully conforms of the results of the samples after soaking process with the results of the samples before soaking. The data and the valuations of the peaks tell us that may be appearances for peaks belong to the bone-like apatite

(mainly HA) located underneath the peak positioned at 958.30 cm<sup>-1</sup> in this sample after soaking in the SBF for one week period as seen from the figure. This may due to the presence of HA in the preparation of the sample.

Table (8) summarized the data of the peaks position collected by Raman spectrum and a comparison between the samples S1 (ALG + BR + WO+HA+TiO<sub>2</sub>) Raman peaks with brushite Raman database indexed by RRUFF database.

Before Soaking		After Soaking	
Wave number (cm <sup>-1</sup> )	Int., %	Wave number (cm <sup>-1</sup> )	Int., %
344.8	31	351.8	31
390.4	60	390.4	60
511.9	36	511.9	36
580.8	30	580.8	30
635.3	97	635.3	97
730.7	43	730.7	43
807.4	43	807.4	43
852.2	20	852.2	20
883.7	38	883.7	38
958.3	100	958.3	100
980.5	43	980.5	43
1046.1	60	1046.1	60

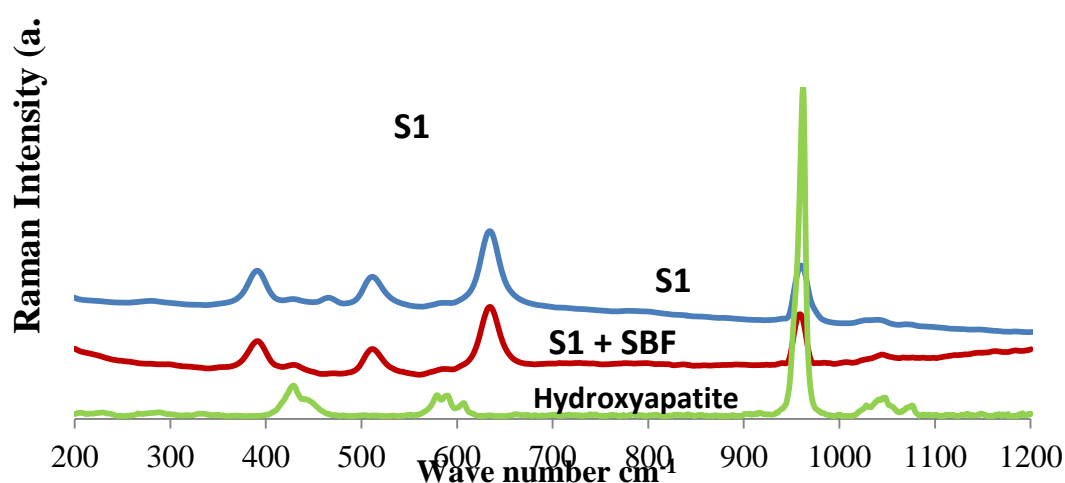


Figure (9): Raman spectrum of Alginate with Brushite cement, Wollastonite, Titanium Oxide and Zinc Oxide (S2) before and after soaking in SBF for one week comparing with the standard database of Hydroxyapatite indexed from RRUFF database.

Figure (9) shows the dependable Raman spectrum of the measured for the sample before, the second due to the soaked sample in SBF and the last for the Hydroxyapatite RRUFF database. Table (9) analyses the Raman peak position and their intensity percentage before and after soaking in SBF. The data belongs to the sample before soaking reveal 10 peaks are observed at 279.5, 391.3, 428.0, 465.6, 510.9, 572.6, 634.3, 765.5, 960.2 and 1040.3  $\text{cm}^{-1}$ , respectively. The peak measured at 391.3  $\text{cm}^{-1}$  is assigned to Wollastonite and/or  $\text{TiO}_2$  (WO at 389.0  $\text{cm}^{-1}$  and 397.0  $\text{cm}^{-1}$ ,  $\text{TiO}_2$ ). The peak at 428.0  $\text{cm}^{-1}$  is belonged to lattice vibration mode of Zinc Oxide (Damen et al., 1966) and the peaks at 465.6 (466.0  $\text{cm}^{-1}$ ) is belong to vibration modes of Wollastonite (Buzatu and Buzgar., 2010), while the peaks positioned at 510.9  $\text{cm}^{-1}$  is assigned to PO bending vibration mode of Brushite and/or  $\text{TiO}_2$ , the peak which located at 572.6  $\text{cm}^{-1}$  is assigned to PO bending mode and the presence of O-Si-O bending of Wollastonite. The peak located at 634.3 is assigned to Si-O of Wollastonite and/or  $\text{TiO}_2$  (Hardcastle, 2011). The peak located at 765.5  $\text{cm}^{-1}$  is assigned for Titanium Oxide. The peaks at 960.2  $\text{cm}^{-1}$  is assigned to Si-O for Wollastonite, brushite and / or PO stretching mode of Hydroxyapatite. The peaks located at 279.5  $\text{cm}^{-1}$  is not identified till know (to our knowledge) and need more evaluation. To read more about symmetry and ant-symmetry vibration modes of titanium oxide and Zn O refer to (Ishioka and Petek, 2012) and (Jabri, et al. 2015).

Data collected after soaking the sample for a period of one week in the SBF revealed that the disappearance of three peaks are located at 279.5, 465.6 and 765.5  $\text{cm}^{-1}$ . These peaks might disappear owing to the interaction between the sample elements and the chemical components of the SBF. The data and the assessments of the peaks of the spectrum reveal that there are appearances for many peaks such as 424.8, 572.6 and 960 that could be concealed beneath bone-like apatite (HA) after soaking the sample for one week in SBF.

**Table (9) summarized the data of the peaks position collected by Raman spectrum and a comparison between the samples S2 (ALG + BR + WO+ $\text{TiO}_2$ +ZnO) Raman peaks with brushite Raman database indexed by RRUFF database.**

Before Soaking		After Soaking	
Wave number ( $\text{cm}^{-1}$ )	Int., %	Wave number ( $\text{cm}^{-1}$ )	Int., %
279.5	5	missed	Missed
391.3	79	391.3	79
428.0	5	428.4	8
465.6	10	missed	missed
510.9	70	511.9	60
572.6	5	581.6	5
634.3	100	634.3	100

Before Soaking		After Soaking	
765.5	5	missed	missed
960.2	81	958.3	90
1040.3	15	1045.1	10

#### IV. Discussion.

The samples under investigation are used to select samples which can be considered suitable as a biomaterial in vitro. The samples prepared in the form of tow samples each one regards with a group of additives including sodium Alginate, Wollastonite, Titanium Oxide, Hydroxyapatite and Zinc Oxide. Soaking brushite samples with their additives in SBF for one week may cause presence of a bone-like apatite layer phase ( $\text{Ca}_{10}(\text{OH})_2(\text{PO}_4)_6$ , HA) on the surface of these samples. To sustain the aim of the study the samples studied by using the X-ray diffraction spectra, scanning electron microscope and Raman spectroscopy. The X-ray diffraction used to ensure the presence of the components used in the preparation of the samples is present in the samples or not. The study of X-ray examination for the samples under investigation after soaking for one week in SBF to help us to recognize new phases appearing after the interaction between the samples surfaces and the components of the SBF. The scanning electron microscope used in two ways. The first was obtaining the SEM images to compare between the changes on the surface of the samples before and after soaking in SBF. The second concern the study of the EDS graphs and hence use the elemental analysis to evaluate the ratio between the presences of Calcium to phosphorus (Ca/P) to recognize the precipitation of bone-like apatite on the surface of the samples. The Raman spectroscopy used to investigate the presence of the chemical functional groups was resulted from the interaction between the samples and the SBF. These results were summarized in table (10) which used to present the chances of formation of hydroxyapatite as a bone-like apatite on the surface of the samples (Yes) means presence of HA and (No) means absence of HA as product after soaking

**Table (10) summarizes the results of the presence of bone-like apatite in the samples under investigation through the study of X-ray diffraction spectra, Raman spectroscopy and EDS data**

Sample	X-ray S (HA)	Raman S (HA)	EDS (Ca/P)
S1	Yes	Yes	1.43
S2	Yes	Yes	1.69

Results were obtained for Sample S1 were studied before and after soaked in SBF, the data were measured before the soaking and compared with the data after soaking. The spectrum of X-ray diffraction of the sample S1 pointed to the presence of many phases lead up to the deposition of bone-like apatite on the sample surface. Raman spectra confirmed that there is non-occurrence of any active chemical groups of facilitating for the deposition process of bone-like apatite on the sample surface. But there are some

peaks which belong to the hydroxyapatite as a bone-like apatite. These data were observed through the study of scanning electron microscopy (SEM) and elemental analysis (EDS) to calculate the ratio between calcium and phosphorus, which equal to 1.43 after soaking. This number is adequate to identify the presence of the hydroxyapatite as type of bone-like apatite listed in table (7). Therefore, all the evidences lead to the identification of sample S1 as an acceptable sample of the biomaterials in vitro.

Sample S2 were studied before and after soaked in SBF, the data measured before the soaking and compared with the data after soaking in SBF. The spectrum of X-ray diffraction of the sample S2 pointed out to the presence of many phases driving to deposition of bone-like apatite on the sample surface. Raman spectra confirmed that there is non-occurrence of any active chemical groups of assisting to the deposition process of bone-like apatite on the sample surface. But there are some peaks which belong to the hydroxyapatite as a bone-like apatite. These data were observed through the study of scanning electron microscopy (SEM) and elemental analysis (EDS) to figure out the ratio between calcium and phosphorus, which equal to 1.69 after soaking. The data is sufficient for identifying the presence of the hydroxyapatite as type of bone-like apatite listed in table (7). Therefore, all the evidences lead to the consistency of sample S2 as a satisfactory sample of the biomaterials in vitro.

## V. Conclusion and Implications.

This current study contributes to the health field for all members of society, including all employees of the Ministry of Education, including employees, teachers and students, as it provides alternatives for bones that are biocompatible such as bone cement and the improvement of its physical properties to be more effective, and this contributes to reducing the material costs of the state in the field of bone substitutes. The study has some limitations i.e., difficulty in obtaining materials to prepare samples, the high financial cost of materials and the difficulty of reaching the nanoscale center in Jeddah and getting an early date, which led to a delay in reaching the results. Future research should focus on adopting this research paper from an official authority so that we can expand the study of samples. Besides, it is recommended to provide permits to obtain materials and study samples on living creatures in specialized scientific centers.

## References.

- Alkhraisat, MH; Cabrejos-Azama, J; Rodríguez, CR; Jerez, LB; Cabarcos, E L. "Magnesium substitution in brushite cements." *Materials Science and Engineering: C*; 2013; 33: 475 – 481.
- Alwahhabi, BK. "Osteoporosis in Saudi Arabia, are we doing enough?" *Saudi Med. J.*; 2015; 36: 1149-1150.
- BarrÈre, F; van Blitterswijk, C; de Groot K. "Bone regeneration: molecular and cellular interactions with calcium phosphate ceramics" *Int J Nanomed*; 2006: 1: 317- 332.

- Buzatu, A and Buzgar, N. "The Raman study of single-chain silicates" *Geologie, tomul*; 2010: 1: 107-125.
- Dabiri, SMH; Lagazzo, A; Farokhi, F; Barberis, M; Finochio, E; Pastorino, LL. "Characterization of alginate-brushite in-situ hydrogel composites" *Materials Science and Engineering: C*; 2016: 67: 502–510.
- Damen, TC; Porto, SPS; Tell B. "Raman effect in Zinc Oxide" *Physical Review*; 1966: 142: 570- 575.
- DiNicolantonio, J. J., Mehta, V., Zaman, S. B., & O'Keefe, J. H. "Not Salt But Sugar As Aetiological In Osteoporosis: A Review". *Missouri medicine*; 2018: 115(3): 247–252.
- Forst RL, Xi Y, Pogson RE, Millar GJ, Tan K, Palmer SJ. "Raman spectroscopy of synthetic CaHPO<sub>4</sub>.2H<sub>2</sub>O and in comparison with the cave mineral brushite" *Journal of Raman spectroscopy*; 2012: 43: 571- 576.
- Gao C, Xu Y, Li L, Gu WQ, Yi CT, Zhu Q, Gu HA, Chen BH, Wang QQ, Tang F, Xu JL, Hou JM, Song HJ, Wang H, Wang ZL, Zhang ZL. "Prevalence of osteoporotic vertebral fracture among community-dwelling elderly in Shanghai". *Chin Med J (Engl)*.; 2019: 132(14):1749-1751.
- Grover, L.M; Knowles, JC; Fleming, GJP; Barralet, JE. "In vitro ageing of brushite calcium phosphate cement" *Biomaterials*; 2003: 23: 4133–4141.
- Hardcastle, FD. "Raman spectroscopy of Titania (TiO<sub>2</sub>) nanotubular water-splitting catalysts" *Journal of the Arkansas Academy Science*; 2011: 65: 43- 48.
- Ishioka, K and Petek H. "Raman generation of coherent phonons of anatase and rutile TiO<sub>2</sub> Photoexcited" *Physical review B*86, 2012: 20520: 1 – 6.
- Jabri, S; Souissi, H; Souissi, A; Meftah, A; Sallet, V; Lusson, A; Galtier P; Oueslati, M." investigation of the vibrational modes of ZnO grown by MOCVD on different orientation planes" *J. Raman Spectrosc.* 2015: 46: 251– 255.
- Jain, D; and Bar-Shalom, D. "Alginate drug delivery systems application in context of pharmaceutical and biomedical research" *Drug Dev Ind Pharm*; 2014: 40: 1576- 1584 ..
- Juhasz, JA; Best, SM; Auffret, AD; Bonfield, W. "Biological Control of Apatite Growth in Simulated Body Fluid and Human Blood Serum" *J. Mater. Sci. Mater. Med.*; 2008: 19: 1823–1829.
- Kokubo, T; and Takadama, H. "How useful is SBF in predicting in vivo bone bioactivity?" *Biomaterials*; 2006: 27: 2907- 2915.
- Kokubo, T; Kushitani, H; Sakka S; Kitsugi, T; Yamamuro, T. "Solutions able to reproduce in vivo surface-structure changes in bioactive glass-ceramic A-W" *J. Biomed. Mater. Res.*; 1990: 24: 721-734.
- Kweon, S. M., Sohn, D. H., Park, J. H., Koh, J. H., Park, E. K., Lee, H. N., Kim, K., Kim, Y., Kim, G. T., & Lee, S. G. "Male patients with rheumatoid arthritis have an increased risk of osteoporosis: Frequency and risk factors". *Medicine*; 2018: 97(24): e11122.

- Madsen, HEL. "Influence of Foreign Metal Ions on Crystal Growth and Morphology of Brushite ( $\text{CaHPO}_4 \cdot 2\text{H}_2\text{O}$ ) and its Transformation to Octacalcium Phosphate and Apatite" J. Cryst. Growth; 2008; 310: 2602–2612.
- Mirza, F., & Canalis, E. "Management of endocrine disease: Secondary osteoporosis: pathophysiology and management". European journal of endocrinology; 2015: 173(3): R131–R151.
- Monma, T; and Kamiya, T. "Preparation of Hydroxyapatite by the Hydrolysis of Brushite" J. Mater. Sci.; 1987: 22: 4247–4250.
- Murat, S., Dogruoz Karatekin, B., Demirdag, F., & Kolbasi, E. N. "Anthropometric and Body Composition Measurements Related to Osteoporosis in Geriatric Population". Medeniyet medical journal; 2021: 36(4): 294–301.
- Olic-Akrapovic, I., Radic, M., & Tonkic, A. "Is there higher percentage of undetected osteopenia and osteoporosis among patients with ulcerative colitis in Saudi Arabia?". World journal of gastroenterology; 2021: 27(27): 4481–4483.
- Pouresmaeili, F., Kamalidehghan, B., Kamarehei, M., & Goh, Y. M. A "comprehensive overview on osteoporosis and its risk factors". Therapeutics and clinical risk management; 2018: 14: 2029–2049.
- Ranter, BD; Hoffman, AS; Schoen, FJ; Lemons, JE. "Biomaterials Science, an introduction to materials in medicine" Academic press, New York 1996.
- Sadat-Ali, M; Al-Habdan, IM; Al-Turki, HA; Azam, MQ. "An epidemiological analysis of the incidence of osteoporosis and osteoporosis-related fractures among the Saudi Arabian population" Ann Saudi Med.; 2012: 32: 637-641.
- Scimeca, M., Centofanti, F., Celi, M., Gasbarra, E., Novelli, G., Botta, A., & Tarantino, U. "Vitamin D Receptor in Muscle Atrophy of Elderly Patients: A Key Element of Osteoporosis-Sarcopenia Connection". Aging and disease; 2018: 9(6): 952–964.
- Tamimi, F; Sheikh, Z; Barralet, J. "Dicalcium phosphate cements: Brushite and monetite" Acta Biomaterialia; 2012: 8: 474 – 487.
- Tas, AC, and Bhadur, SBI. "Chemical Processing of  $\text{CaHPO}_4 \cdot 2\text{H}_2\text{O}$ : It's Conversion to Hydroxyapatite" J. Am. Ceram. Soc.; 2004: 87: 2195–2200.
- Xu, J; Butler, IS; Gilson, DFR. "FT-Raman and high-pressure infrared spectroscopic studies of dicalcium phosphate dihydrate ( $\text{CaHPO}_4 \cdot 2\text{H}_2\text{O}$ ) and anhydrous dicalcium phosphate ( $\text{CaHPO}_4$ )" Spectrochim. Acta Part A; 1999: 55: 2801–2809.